Hindawi
International Journal of Antennas and Propagation
Volume 2022, Article ID 5458069, 8 pages
https://doi.org/10.1155/2022/5458069

Research Article

New Circular-Slot Circularly Polarized Antenna with Modified Characteristic

Lei Wang, Bin Yao, Wenxiao Fang, Chuangmian Huang, Yun Huang, and Yunfei En

Science and Technology on Reliability Physics and Application of Electronic Component Laboratory, CEPREI, Guangzhou, China

Correspondence should be addressed to Lei Wang; leiwang@ceprei.com and Chuangmian Huang; huangchuangmian@163.com

Received 29 January 2022; Revised 30 March 2022; Accepted 4 April 2022; Published 22 April 2022

Academic Editor: Paolo Burghignoli

In this article, a novel broad circularly polarized antenna (CPA) with circular-slot ground is presented. The circular-slot CPA is consisted of a circular-slot ground, an I-shaped slit and a semicircle loop feeding structure. By using semicircle loop feeding structure and adding a slit into the circular-slot ground as perturbation elements, the multiple CP resonant modes could be stimulated simultaneously. To demonstrate to the design radiational, an antenna model was printed, manufactured, and tested. The tested results reveal that the proposed antenna has a broad 3-dB ARBW of $|S_{11}| < -10$ dB that could be obtained, which is suitable for the application of wireless communication systems.

1. Introduction

In modern communications such as wireless local area networks systems (WLANs/WiMAX) and avigation satellite systems (GPS/BDS/GLONASS), circularly polarized antenna (CPA) has attracted increasing attention because of its significant merits of suppressing multipath effects and minimizing polarization mismatch between a transmitter and receiver. In addition, broad planar slot antenna is one of the promising candidates in the design of CPAs owing to their broad impedance bandwidth (IBW), low cost and profile, and easy integration with circuits. Recently, many wide slot CPAs using different slot structures have been extensively studied in [1–22] for the purpose of meeting the demand of wideband operation. Among them, etching circular or square slots into the ground planes is one of the most popular methods for enhancing bandwidth. Based on the circular-slot ground, various different feeding structures [2–5] are introduced into the design of slot CPAs. Ref. 2 introduces a microstrip feedline with semicircular patch into the circular-slot ground plane to obtain 58.7% 3-dB axial ratio bandwidth (ARBW). Based on the semicircular feeding structure, a curved slot is etched into the circular-slot ground plane to achieve dual-band dual-sense CP operation in [3]. Similarly, a C-shaped slotted patch and a pair of perturbation slots are introduced into the circular-slot ground plane in [4, 5], which realize 91% and 76.6% 3-dB ARBW, respectively. Besides, based on the square slot ground, several slot CPAs are also extensively studied in [1, 6–8]. For example, through introducing a T-shaped strip and spiral slots into the square slot ground, a broad slot CPA [1] could realize wide 3-dB ARBW of 56%. Similarly, square patch [6], arc-shaped strip [7], inverted-L strips [8, 9], I-shaped strips [10], protruded strip [11], and spiral slots [12] as perturbation elements are inserted into the square slot ground to obtain broad 3-dB ARBW of 6%, 18.8%, 25%, 48.8%, 30%, 52%, and 56%, respectively. The reason for the increase in bandwidth is that the parasitic perturbation elements could generate a new current path, which results in the exciting of the additional CP resonant mode.

In this article, based on reviewing the literature, a novel broadband CPA with circular slot ground is presented. By using semicircle loop feeding structure and adding a slit into the circular-slot ground, the broad 3-dB ARBW of $|S_{11}| < -10$ dB could be obtained. The presented slot CPA is printed, manufactured, and measured. Tested results reveal that the 3-dB ARBW is 60% from 2.6 to 3.6 GHz, which is superior than [1, 6–11]. The main content of this article includes analysis of four evolutionary models and surface current distribution, parametric investigation, and the

discussion of simulated and measured results. In addition, a comparison between the presented slot CPA and other referenced slot CPAs is listed in Table 1, which indicates that the proposed slot CPA features a significant characteristic of wider CPBW.

2. Antenna Design and Configuration

Geometry of the designed CPA with circular slot ground is plotted in Figure 1. As seen, the slot CPA is etched on a substate with a dielectric constant of 3.35 and heigh of 0.8 mm. The designed slot CPA includes a semicircle loop feeding structure ($L1 \times W1$, $L2 \times W2$, and $R1 \times R2$), an I-shaped strip ($L3 \times W3$) as perturbation element, and a circular-slot ground plane ($L \times W \times$ R). Firstly, the semicircle loop feeding structure is used to improve the impedance match and provide an excited resource. Secondly, the circular slot is embedded in the ground plane to provide current path of exciting CP mode. Thirdly, the I-shaped strip is inserted into the circular-slot ground to tune the AR resonant point and impedance match. Finally, multiple AR resonant points were stimulated simultaneously using modified feeding structure and slots as perturbation elements. The designed slot CPA is printed and manufactured and measured to prove the rationality of the design. The measured results show thst the 3-dB ARBW is 98.2% from 2.42 GHz to 6.8 GHz within the −10-dB IBW.

3. Antenna Analysis and Discussion

To analyze the underlying operated mechanism of slot CPA, four evolutionary models with different structures are depicted in Figure 2. The corresponding $|S_{11}|$ and AR values are plotted together in Figure 3. Firstly, for a conventional ring slot, the dominant resonant mode is a TE_{11} mode and it occurs at [21]:

$$f_{TE_{11}} \approx \frac{1.84c}{2\pi R} \times \frac{1}{\sqrt{\varepsilon_r}}, \quad (1)$$

where c equals 3×10^8 m/s, ε_r is the dielectric constant of the substrate, and R is the radius of the slot. Using equation (1), the calculated cut-off frequency occurs at approximately 2.7 GHz.

However, the surface current of the I-shaped strip and sector feeding structure is opposite to that of the slot ground plane in this manuscript, which causes the cut-off frequency to shift to high frequency, as shown in Figure 3. These antenna models are presented as below: Ant. 1 consisting of a circular-slot ground and a sector feeding structure has bad $|S_{11}|$ and AR values. When the sector feeding structure is replaced with the semicircle loop feeding structure in Ant. 2, the ARBW could be significantly improved, whereas there is no obvious change in IBW. To improve the impedance match, the semicircle loop is moved to the excited port by a distance of D in Ant. 3. It is obviously observed that the IBW and ARBW have extensive improvement and a new AR resonant point occurs at high-frequency (6.2 GHz). However, in this case, the IBW of Ant. 3 cannot completely cover the ARBW in low frequency. Therefore, to further improve the IBW, a tuned I-shaped strip as perturbation element is inserted into the circular-slot ground in the proposed antenna. As seen, the IBW and ARBW of the proposed antenna could be enhanced in low frequency. This is because that the introduction of the I-shaped strip could increase the current path, which results in the shift of the resonant point to low frequency. Finally, the proposed antenna has a wider 3-dB ARBW which is 98.2% from 2.42 GHz to 6.8 GHz within the -10 dB IBW.

To reveal the CP operation mechanism of the slot CPA, the vector surface current distributions with simulated way at two AR resonant points (3.45 and 5.1 GHz) are plotted in Figures 4(a) and 4(b). As seen, the surface currents are mainly concentrated on the semicircle loop feeding structure ($J3$) and L-shaped strip ($J4$), whereas a small part distributes on the circular-slot ground plane ($J1$ and $J2$). With respect to the circular-slot ground, it is observed that the sum of surface currents $J1$ and $J2$ at low frequency (3.45 GHz) is orthogonal with different phases (phi = 0° and phi = 90°), which means that the circular-slot ground could excite a CP resonant mode alone. However, it is reversed at high frequency (5.1 GHz). In addition, the surface current on the I-shaped strip at low frequency is stronger than that at high frequency, which reveals that the I-shaped strip plays a role on CP radiation at low frequency. Finally, the total surface current (J) is orthogonal and rotates counterclockwise with different phases at both low and highfrequencies, which indicates that the designed slot CPA could stimulate right-hand circular polarization (RHCP) wave at low and high frequencies in $+z$-direction. At last, two different resonant modes at 3.45 and 5.1 GHz can also be observed in Figure 4. As seen, the quasi-TE_{11} mode and quasi-TE_{21} mode are excited in the circular aperture at 3.45 GHz and 5.1 GHz, respectively.

To analyze the impact of these perturbation strips on the IBW and ARBW, multiple parameters are simulated and scanned by using the single variable method. These variable parameters comprise the radius of circular slot (R) and semicircle loop feeding structure ($R1$), the length of I-shaped strip ($L3$), and the distance (D) between the centers of the circular slot and the loop. The corresponding return loss and AR values are depicted in Figures 5(a)–5(d). As seen, the parameters R and D have a significant impact on the IBW and ARBW at the entire frequency, while the $R1$ and $L3$ obviously impact the performance of antenna at low frequency. The reason for this phenomenon is that the circular-slot ground and semicircle loop are the main driven element, whereas the I-shaped strip is the parasitic element as perturbation strip. The best CP performance could be realized when $R = 17.8$ mm, $R1 = 2.8$ mm, $L3 = 7.8$ mm, and $D = 7$ mm are set. Finally, the dimensions of the proposed antenna are shown in Table 2.

4. Experimental Results

In this section, an antenna prototype was simulated, printed, and measured to demonstrate the design rationality. A vector network analyzer is used to measure the $|S_{11}|$ values,

Table 1: Comparison of the proposed antenna to previously reported antennas.

Antenna	Type	−10 dB IBW	3-dB ARBW	CPBW	Antenna size	Total gain (dBic)
[2]	Single-layered	111.6	58.4	58.4	$0.71\lambda_0 \times 0.71\lambda_0 \times 0.02\lambda_0$ at 5.685 GHz	6.18
[11]	Single-layered	101.3	52%	52%	$1.20\lambda_0 \times 1.20\lambda_0 \times 0.032\lambda_0$ at 6 GHz	8.6
[12]	Single-layered	>110%	56%	56%	$0.40\lambda_0 \times 0.40\lambda_0 \times 0.016\lambda_0$ at 6 GHz	8.6
[13]	Single-layered	65.8%	75.1%	65.8%	$0.80\lambda_0 \times 0.80\lambda_0 \times 0.016\lambda_0$ at 6 GHz	4.6
[14]	Single-layered	92.7%	54.2%	54.2%	$0.80\lambda_0 \times 0.80\lambda_0 \times 0.016\lambda_0$ at 6 GHz	4.5
[18]	Single-layered	62%	49%	49%	$0.54\lambda_0 \times 0.57\lambda_0 \times 0.015\lambda_0$ at 6 GHz	3.5
[20]	Single-layered	87.8%	96%	87.8%	$0.80\lambda_0 \times 0.80\lambda_0 \times 0.016\lambda_0$ at 6 GHz	4.75
This work	Single-layered	110.0%	75.7%	75.7%	$1.0\lambda_0 \times 1.0\lambda_0 \times 0.016\lambda_0$ at 6 GHz	4.52

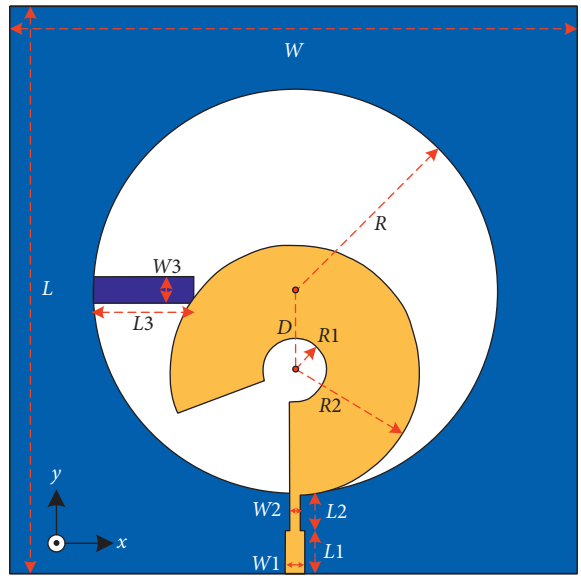

Figure 1: Geometry of the designed slot CPA.

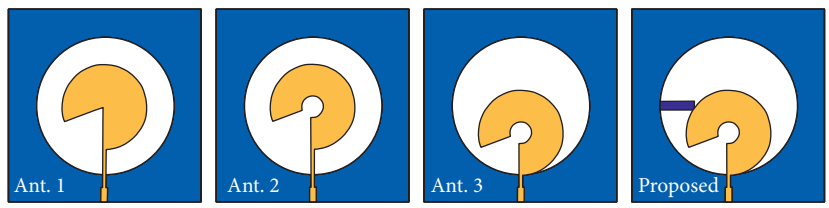

Figure 2: Four evolutionary models with different structures.

and the Satimo Starlab measurement system is utilized to test the AR, gain, and radiation pattern values. The corresponding curves are shown in Figures 6 and 7, respectively. The simulated impedance bandwidth (IBW, $|S_{11}| < -10$ dB) and 3-dB ARBW are 114.6% (2.85–10.50, 6.675 GHz) and 76.9% (3.00–6.75, 4.875 GHz), while the measured results are 110.0% (3.05–10.50, 6.775 GHz) and 75.7% (3.02–6.70, 4.86 GHz). In addition, the measured and simulated total gains are 4.52 and 4.90 dBic, respectively. Finally, to study the direction of the designed antenna, the tested and simulated normalized radiation pattern values in E-planes and H-planes at two frequency points (3.45 and 5.10 GHz) are depicted in Figures 8(a) and 8(b). As depicted, the LHCP values are smaller than the RHCP parts by 18 dB, which means that the designed antenna could excite RHCP waves in $+z$ direction. In addition, it is noticed that the antenna is bidirectional due to the circular-slot ground participating in the radiation.

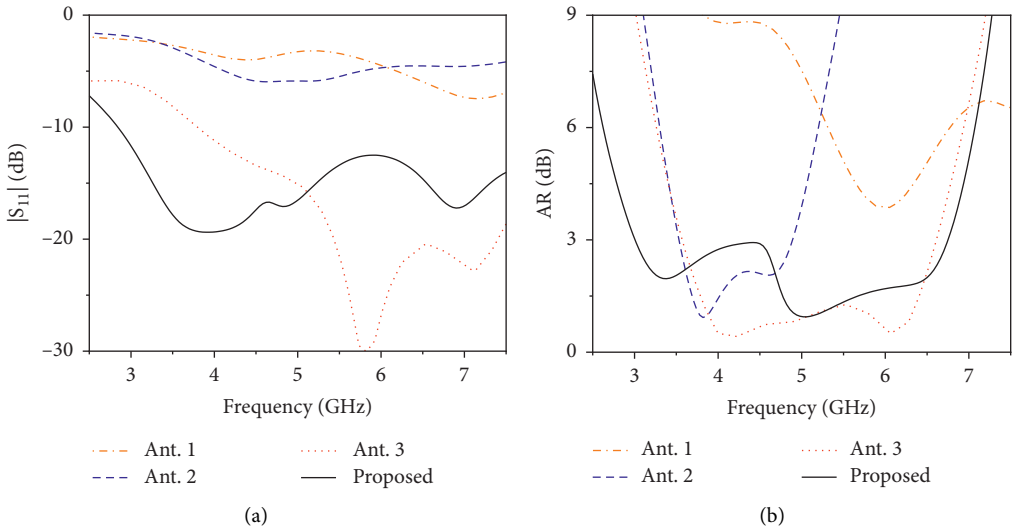

Figure 3: Results for four evolutional models. (a) $|S_{11}|$ curves. (b) AR curves.

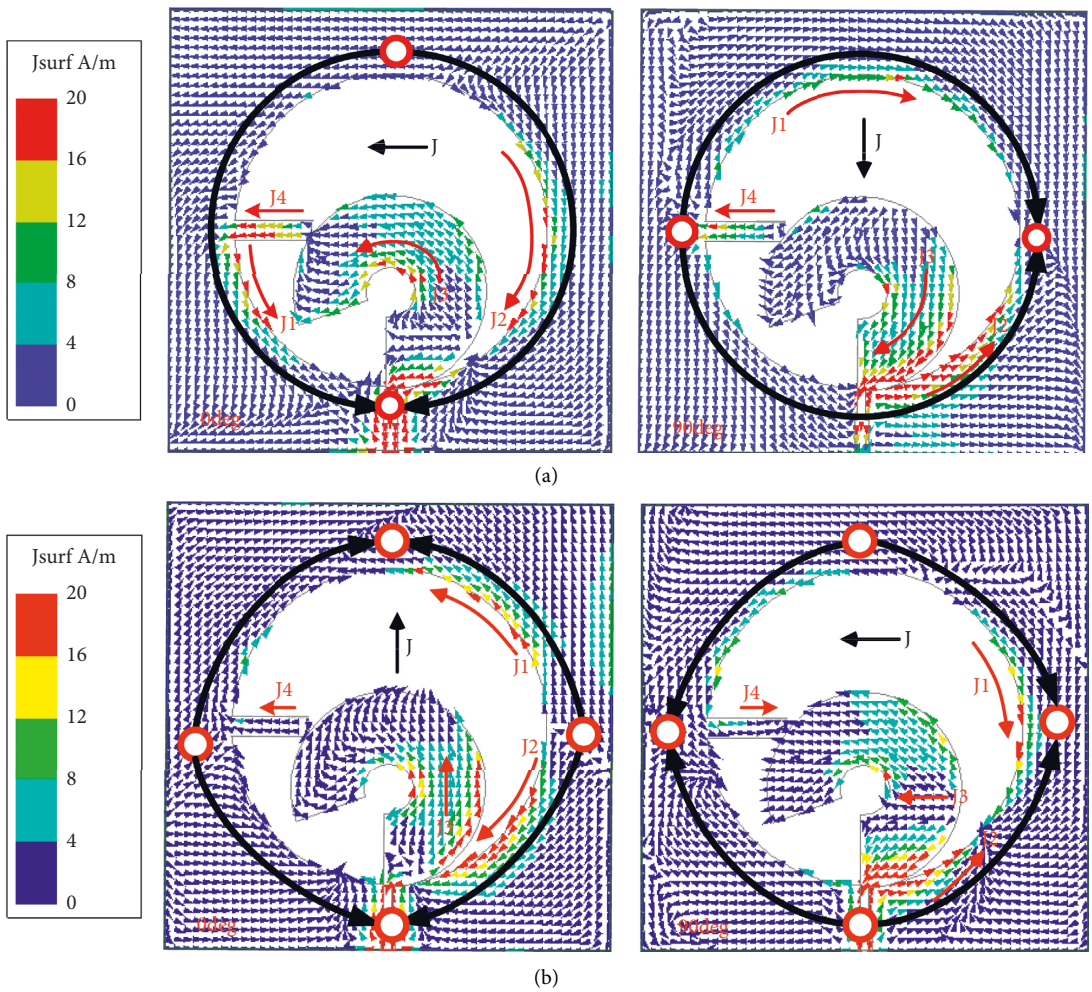

Figure 4: Simulated surface current distributions of the proposed antenna at (a) 3.45 GHz and (b) 5.1 GHz.

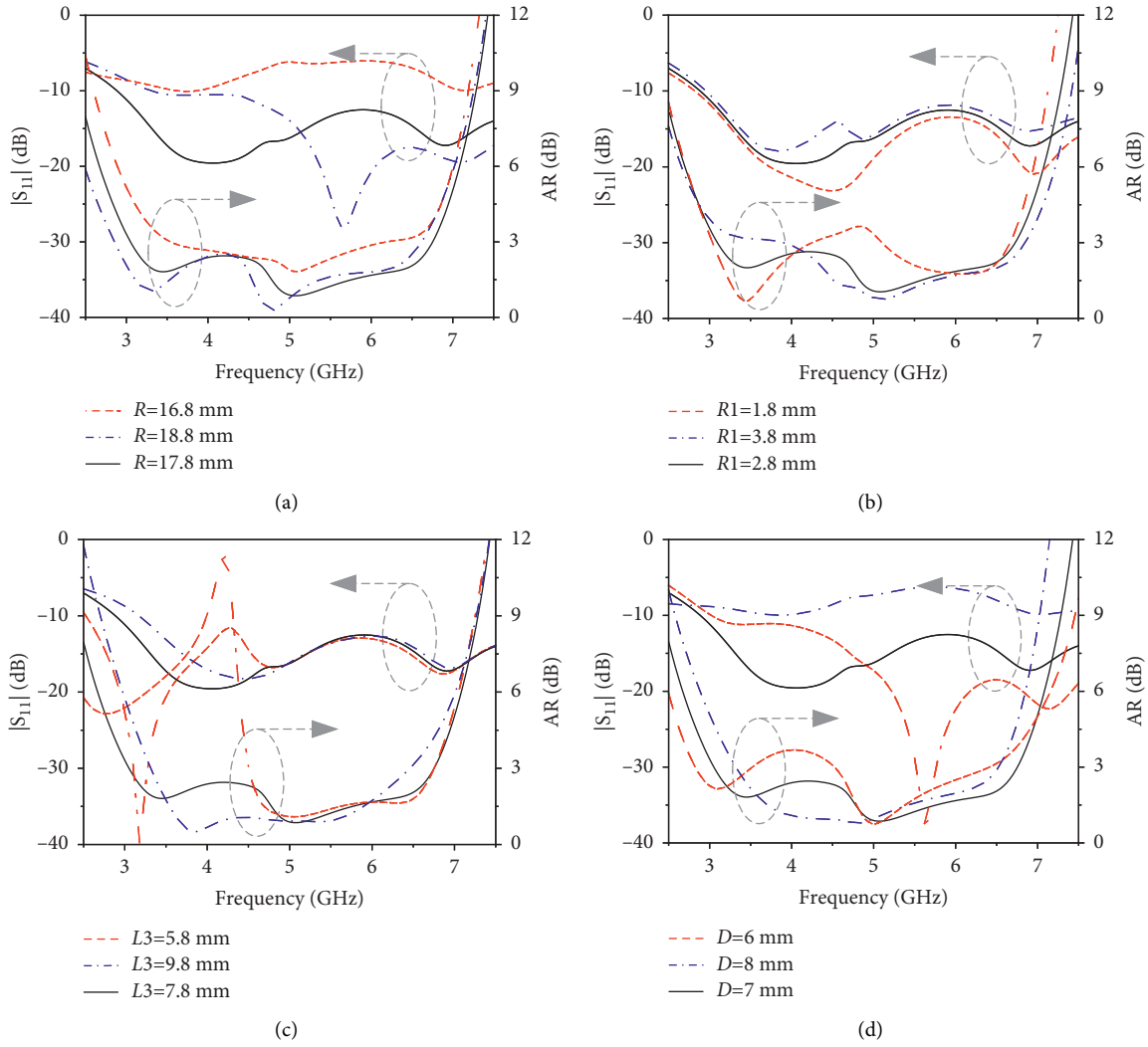

Figure 5: Impact of changing parameters on the $|S_{11}|$ and the AR values, (a) R, (b) $R1$, (c) $L3$, and (d) D.

Table 2: Dimensions of the presented antenna.

Parameters	Values (mm)
L	50
$L1$	3.8
$L2$	3.2
$L3$	7.8
D	7.0
$R1$	2.8
W	50
$W1$	1.6
$W2$	0.9
$W3$	2.2
R	17.8
$R2$	11.0

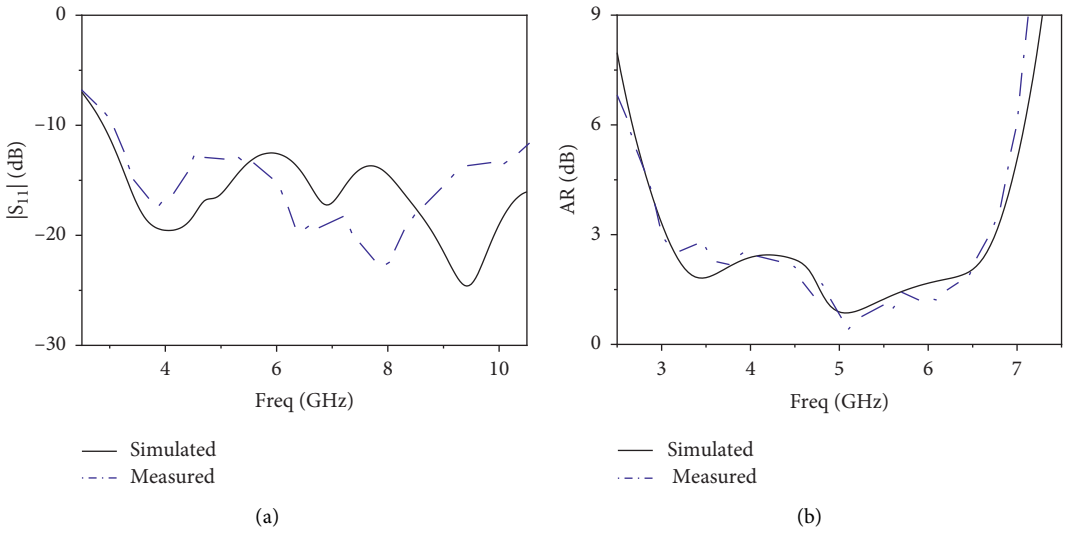

Figure 6: Simulated and tested $|S_{11}|$ and AR results of the CPMA. (a) $|S_{11}|$ curves and (b) AR curves.

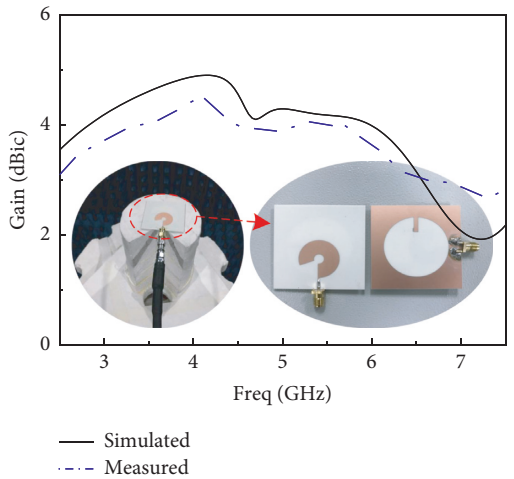

Figure 7: Simulated and tested gain curves and measurement photos of the CPMA.

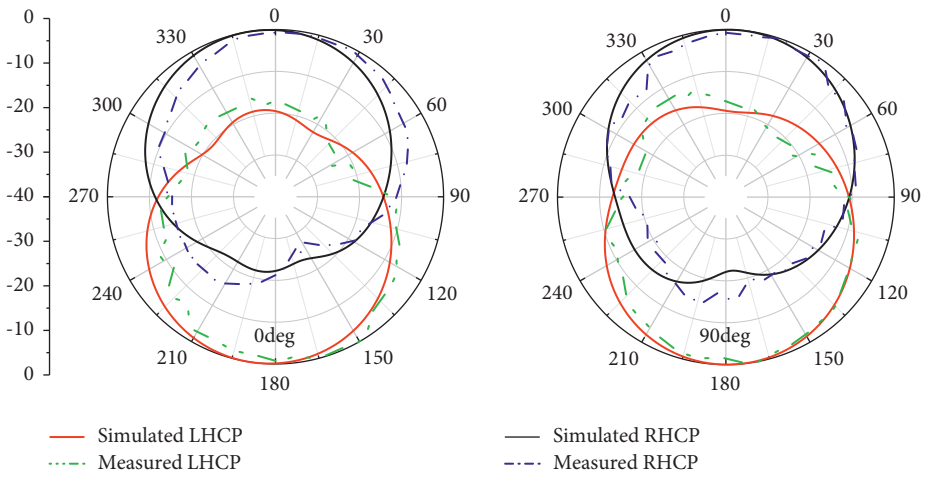

(a)

Figure 8: Continued.

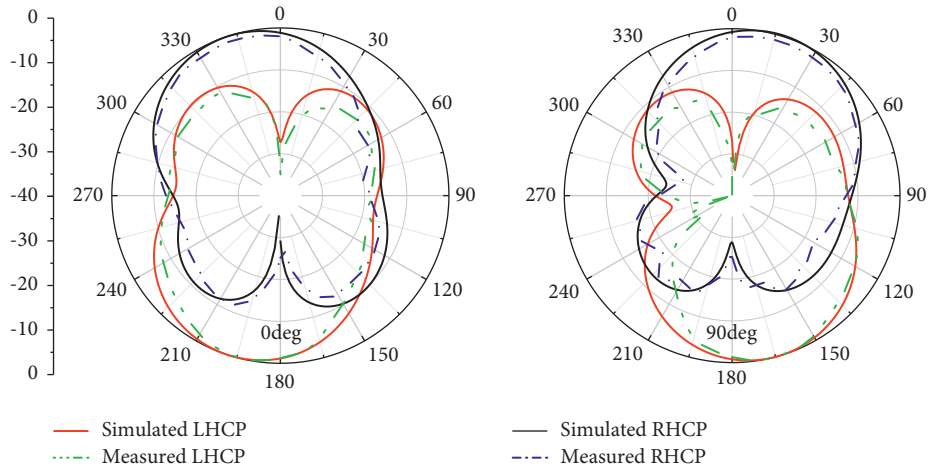

(b)

Figure 8: Simulated and tested normalized radiation patterns with different frequency points at (a) 3.45 GHz and (b) 5.10 GHz.

5. Conclusions

In this article, a novel broad CPA with circular-slot ground is presented. The circular-slot CPA is consisted of a circular-slot ground, an I-shaped slit and a semicircle loop feeding structure. Multiple CP resonant modes could be stimulated simultaneously by combining the semicircle loop feeding structure with the circular-slot ground loaded with an I-shaped slit as perturbation elements. To demonstrate to the design radiational, an antenna model was printed, manufactured, and tested. There is a good consistency between the simulated and tested values. The tested results reveal that the proposed antenna has a broad 3-dB ARBW of $|S_{11}|<-10$ dB that could be obtained, which is suitable for the application of wireless communication systems.

Data Availability

The data used to support the findings of this study are available from the corresponding author upon request.

Conflicts of Interest

The authors declare that they have no conflicts of interest.

References

[1] C. Chen and E. K. N. Yung, "Dual-band dual-sense circularly-polarized CPW-fed slot antenna with two spiral slots loaded," *IEEE Transactions on Antennas and Propagation*, vol. 57, no. 6, pp. 1829–1833, 2009.

[2] T. Tuan Le, V. Hoang The, and H. Chang Park, "Simple and compact slot-patch antenna with broadband circularly polarized radiation," *Microwave and Optical Technology Letters*, vol. 58, no. 7, pp. 1634–1641, 2016.

[3] H. H. Tran, T. T. Le, and T. K. Nguyen, "Dual-band dual-sense circularly polar-ized antenna for S- and C-band applications," *Microwave and Optical Technology Letters*, vol. 1–6, 2018.

[4] H. H. Tran, N. Nguyen-Trong, and A. M. Abbosh, "Simple design procedure of a broadband circularly polarized slot monopole antenna assisted by characteristic mode analysis," *IEEE Access*, vol. 6, pp. 78386–78393, 2018.

[5] Y. X. Zhang, Y. C. Jiao, Z. Zhang, and B. Li, "Miniaturised CP aperture antenna with tri-mode operation for broadening bandwidth," *Electronics Letters*, vol. 54, no. 3, pp. 122–124, 2018.

[6] J.-S. Row, "The design of a squarer-ring slot antenna for circular polarization," *IEEE Transactions on Antennas and Propagation*, vol. 53, no. 6, pp. 1967–1972, 2005.

[7] M.-J. Chiang, T.-F. Hung, and S.-S. Bor, "Dual-band circular slot antenna design for circularly and linearly polarized operations," *Microwave and Optical Technology Letters*, vol. 52, no. 12, pp. 2717–2721, 2010.

[8] J. Y. Sze and C. C. Chang, "Circularly polarized square slot antenna with a pair of inverted-L grounded strips," *IEEE Antennas and Wireless Propagation Letters*, vol. 7, pp. 149–151, 2008.

[9] J. Y. Sze, C.-I. G. Hsu, Z. W. Chen, and C. C. Chang, "Broadband CPW-Fed circularly polarized square slot antenna with lightening-shaped feedline and inverted-L grounded strips," *IEEE Transactions on Antennas and Propagation*, vol. 58, no. 3, pp. 973–977, 2010.

[10] J.-Y. Sze, J.-C. Wang, and C.-C. Chang, "Axial-ratio bandwidth enhancement of asymmetric-CPW-fed circularly-polarised square slot antenna," *Electronics Letters*, vol. 44, no. 18, pp. 1048-1049, 2008.

[11] Z.-F. Chen, B. Xu, J. Hu, and S. He, "A CPW-fed broadband circularly polarized wide slot antenna with modified shape of slot and modified feeding structure," *Microwave and Optical Technology Letters*, vol. 58, no. 6, pp. 1453–1457, 2016.

[12] C. Ghobadi, J. Nourinia, and P. Sadeghi, "Square slot antenna with two spiral slots loaded for broadband circular polarisation," *Electronics Letters*, vol. 52, pp. 787-788, 2016.

[13] Y. Liu, S. T. Cai, X. M. Xiong, W. J. Li, and J. Yang, "A novel wideband circularly polarized modified square-slot antenna with loaded strips," *International Journal of RF and Microwave Computer-Aided Engineering*, vol. 29, Article ID e21873, 2019.

[14] L. Wang, W. X. Fang, Y. F. En, Y. Huang, W. Shao, and B. Yao, "A new broadband circularly polarized square-slot antenna with low axial ratios," *International Journal of RF and*

Microwave Computer-Aided Engineering, vol. 29, Article ID e21502, 2019.

[15] K. Saraswat and A. R. Harish, "Analysis of wideband circularly polarized ring slot antenna using characteristics mode for bandwidth enhancement," *International Journal of RF and Microwave Computer-Aided Engineering*, vol. 28, no. 2, Article ID e21186, 2018.

[16] M. Nosrati and N. Tavassolian, "Miniaturized circularly polarized square slot Antenna with enhanced axial-ratio bandwidth using an antipodal Y-strip," *IEEE Antennas and Wireless Propagation Letters*, vol. 99, p. 1, 2016.

[17] R. Xu, J.-Y. Li, J. Liu, S.-G. Zhou, K. Wei, and Z.-J. Xing, "A simple design of compact dual-wideband square slot antenna with dual-sense circularly polarized radiation for WLAN/Wi-Fi communications," *IEEE Transactions on Antennas and Propagation*, vol. 66, no. 9, pp. 4884–4889, 2018.

[18] U. Ubaid and S. Koziel, "A broadband circularly polarized wide-slot antenna with a miniaturized footprint," *IEEE Antennas and Wireless Propagation Letters*, vol. 17, no. 12, pp. 2454–2458, 2018.

[19] T. T. Le, H. H. Tran, and H. C. Park, "Simple-structured dual-slot broadband circularly polarized antenna," *IEEE Antennas and Wireless Propagation Letters*, vol. 17, no. 3, pp. 476–479, 2018.

[20] L. Wen-Wen, Z.-H. Cao, and Z. Wang, "New broadband circularly polarized antenna with an inverted F-shaped feedline," *International Journal of RF and Microwave Computer-Aided Engineering*, vol. 30, Article ID e22313, 2020.

[21] M. S. Ellis, F. Effah, A. R. Ahmed et al., "Asymmetric circularly polarized open-slot antenna," *International Journal of RF and Microwave Computer-Aided Engineering*, vol. 30, Article ID e22141, 2020.

[22] H. F. Huang and Z. P. Zhang, "A small single fed broadband circularly polarized slot antenna," *International Journal of RF and Microwave Computer-Aided Engineering*, vol. 29, Article ID e22122, 2020.